Are Crystal Polymorphs Predictable? The Case of Sexithiophene

Raffaele Guido Della Valle,* Elisabetta Venuti, and Aldo Brillante

Dipartimento di Chimica Fisica e Inorganica and INSTM-UdR Bologna, Universita di Bologna, Viale Risorgimento 4, I-40136 Bologna, Italy

Alberto Girlando

Dipartimento di Chimica GIAF and INSTM-UdR Parma, Universita di Parma, Parco Area delle Scienze, I-43100 Parma, Italy

Received: February 28, 2008; Revised Manuscript Received: April 15, 2008

Using sexithiophene as a benchmark compound, we present a very effective strategy for searching the potential energy minima of a crystalline material, described in terms of rigid molecules with Coulombic and atom−atom interactions. The strategy involves uniform sampling of the many-body energy hypersurface, mechanical identification of all constraints deriving from the crystallographic symmetry, and a "sight−resight" method, originally introduced in wildlife ecology, for assessing the completeness of the search. Thousands of distinct potential energy minima, with a surprising variety of structural arrangements, are identified for sexithiophene. Despite the large number of competing minima, the system presents a small number of deep minima, with very different structures and not particularly congested in energy or density. The two deepest minima correspond to the structures of the two known experimental polymorphs, which are satisfactorily described.

1. Introduction

Organic semiconductors are currently an object of considerable interest for possible applications in molecular electronics.[1,2] The observation that polymorphism is a common feature of organic crystals[3–6] and that charge-transport properties are related to the crystal structure[7–10] has prompted us to investigate the possible occurrence of polymorphs in various molecular semiconductors. For this purpose, we have developed a very effective research strategy,[11–15] which combines experimental and theoretical methods. Experimentally, we mainly use Raman spectroscopy in the region of lattice phonons (10−150 cm^{-1}), which, being very sensitive to the details of the molecular packing in the individual lattice, effectively connects the structural and dynamical properties of the crystal. Raman and micro-Raman spectroscopy allows us to distinguish the various polymorphs, not only as single crystals but even as microdomains (physical impurities), which may be mapped with spatial resolutions reaching 1 μm.[13] Theoretically, once the crystals are described in terms of rigid molecules interacting through a model potential, we start from all available X-ray structures and identify the corresponding local minima of the potential energy. Since these minima represent the possible configurations of mechanical equilibrium and thus constitute the "natural" or "inherent" structures that the system can exhibit,[16] this *local stability* information allows us to discover which of the various observed structures correspond to genuinely distinct polymorphs. Finally, we systematically sample the potential energy hypersurface to check the *global stability* of the observed structures and to investigate the possible occurrence of further polymorphs.

We have already completed this combined strategy for two prototypical organic semiconductors, namely, pentacene[11–13] and tetracene,[14,15] with remarkable success. We theoretically predicted a surprisingly large number of possible polymorphs,[12,15] and, for both compounds, we discovered that the numerous X-ray structures converge either to the first or to the second deepest minimum and thus correspond to the two most stable polymorphs.[11,14] For both pentacene and tetracene, we experimentally confirmed the existence of two distinct polymorphs by identifying two different crystal morphologies, characterized by clearly different Raman spectra in the region of the lattice phonons.[14,17] In the case of pentacene, we also verified the identity of the samples with powder X-ray diffraction measurements,[18] and investigated possible physical impurities by confocal Raman mapping.[13] The existence of both crystalline polymorphs, which had been a matter of discussion,[6,19] has been recently confirmed by single-crystal X-ray diffraction.[20]

Encouraged by these good results, we have tackled the case of α-sexithiophene (α-6T), another very promising semiconducting material. Also for α-6T the X-ray diffraction experiments have identified two crystalline polymorphs. The first is the "low-temperature" (LT) polymorph with four molecules in the unit cell ($Z = 4$), described in an early work by Porzio et al.[21] and revised by Horowitz et al.[22] The second is the "high-temperature" (HT) polymorph with $Z = 2$ identified by Siegrist et al.[23] Both polymorphs are monoclinic and may be described in the space group $P2_1/c$, although equivalent descriptions as $P2_1/n$ or $P2_1/a$ were chosen in the original literature.[21–23] It should be noticed that $P2_1/c$ is a centrosymmetric group and that in the HT form the molecules reside on inversion sites, in agreement with the usual rule[24–26] that molecular inversion symmetry is normally retained in crystals. However, this is not the case for the LT form, which is an exceptional case where the molecules reside on generic sites.

In a recent paper[27] on α-6T we presented polarized Raman spectra and lattice dynamics calculations for the lattice phonons of the two polymorphs. The resulting symmetry assignment of the phonons allowed us to associate each spectrum to the appropriate polymorph, previously identified only by X-ray diffraction.[21–23] Theoretically, we found that the two published LT structures[21,22] ($Z = 4$) fall in the same local minimum of

* Corresponding author.

10.1021/jp801749n CCC: $40.75
Published on Web 07/01/2008

the potential energy, thus confirming that they correspond to the same polymorph. The HT structure[23] ($Z = 2$) falls into a different minimum, as expected. Once accounted for the effects of pressure and temperature by computing the Gibbs energy $G(T,p)$ with quasi-harmonic lattice dynamics (QHLD) methods,[28] the calculations for the two polymorphs[27] described very well the experimental crystal structures and phonon frequencies.

In this paper we complete our project for α-6T, by exploring the potential energy hypersurface. Beside our specific interest for α-6T, we have used this compound as a benchmark to improve and test our search methods. These methods include optimally uniform low-discrepancy sampling of the configuration space, fully automatic identification of the constraints arising from space group and site group symmetries, efficient generation of the molecular orientations, and a strategy for assessing the completeness of the search.

2. Methods

2.1. Quantum Mechanical Calculations. Following our now standard theoretical procedure,[12,15] we started our calculations by determining the ab initio molecular geometries and atomic charges for the isolated α-6T molecule. This was done with the Gaussian03 program,[29] using the B3LYP/6-31G* combination of density functional and basis set.[29,30] In the geometry optimization, the α-6T molecule was maintained planar with symmetry C_{2h}. This choice is justified by the experimental evidence that the α-6T molecule barely deviates from planarity in the X-ray crystal structures.[21–23] In the HT structure,[23] moreover, the molecules lie on crystal inversion centers, compatible only with a centrosymmetric molecular geometry. The atomic charges were determined through a "RESP" fit[31] to the ab initio electrostatic potential (ESP). In a RESP (restrained ESP) fit[31] the charges are restrained toward an "optimal" value of zero. The restraints reduce the magnitude of charges on buried atoms, which are not well determined by the ESP and which often assume unreasonably large values in standard unrestrained "ESP" fits.

2.2. Potential Model. The intermolecular potential was described by the AMBER model,[32,33] in which intermolecular interactions are represented by an atom−atom potential with electrostatic and Lennard-Jones terms, $\Phi_{ij}(r) = q_i q_j/r + 4\varepsilon_{ij}[(\sigma_{ij}/r)^{12} - (\sigma_{ij}/r)^6]$. The parameters σ_{ij} and ε_{ij} depend on the AMBER type of the atoms, which describe atomic species and local coordination. Only "diagonal" σ_{ii} and ε_{ii} parameters are actually specified in the model, since parameters σ_{ij} and ε_{ij} involving unlike types i and j are given by mixing rules $\sigma_{ij} = (\sigma_{ii} + \sigma_{jj})/2$ and $\varepsilon_{ij} = (\varepsilon_{ii}\varepsilon_{jj})^{1/2}$. The atomic charges q_i are the previously discussed RESP charges,[31] evaluated at the B3LYP/6-31G* level,[29] as required by the AMBER protocol.[33] The convergence of the long-range electrostatic interactions was accelerated with Ewald's method.[34,35]

2.3. Choice of Initial Structures. In our previous searches[12,15,36] initial crystal structures were generated without symmetry constraints (space group $P1$), by independently varying the unit cell axes a, b, c and angles α, β, γ, together with the positions and orientations of a given number Z of molecules (described by the coordinates $\mathbf{T}_i$ of their centers of mass and by suitable rotation matrices $\mathbf{R}_i$, with $i = 1, 2,..., Z$). The actual space group was then determined *a posteriori* by analyzing the final structures after energy optimization. Given enough computer time, this strategy certainly saturates the search space, but it is inefficient since high-symmetry structures with $Z \geq 2$ are encountered very rarely.[36] To lessen this problem, we have now searched again for $P1$ structures with $Z = 1$ and 2 and then also searched in the space groups most frequently found in the statistical surveys on the experimental structures of molecular crystals.[26,37,38] For this purpose, we have written a program able to generate structures in any chosen arrangement, given the molecular geometry, the space group, the number Z' of symmetry-independent molecules and their Wyckoff positions[39] in the unit cell. Given only this information, the program derives a set of constraints, which have to be satisfied while generating the initial structures and which must be propagated and maintained during the energy minimization. The constraints concern the lattice parameters a, b, c, α, β, γ and the molecular positions and orientations $\mathbf{T}i$ and $\mathbf{R}i$, with $i = 1, 2,..., Z'$. By reducing the dimensionality of the search space, the constraints greatly increase the search efficiency.

Once the constraints are obtained, the program generates structures by sampling all independent parameters in their allowed ranges. Since random sampling often exhibits gaps and clusters of points, which may be wasteful of computer time, we instead follow a low-discrepancy Sobol' sequence,[40,41] which ensures more uniform, and thus more efficient, distributions. When the energy depends most strongly on a subset of the structural parameters, low-discrepancy sequences are also superior to multidimensional grids, since their uniformity properties survive projection on subspaces of reduced dimensionality.[42]

2.4. Identification of Constraints. The constraints on the lattice parameters, e.g., $\alpha = \gamma = 90°$ for monoclinic systems, are directly derivable from the space group, by examining a short list of cases. Exploiting the space group symmetry to obtain all Z molecules in the unit cell from the smaller set of Z' molecules in the asymmetric unit is also easy. Finding the constraints on the molecular displacements (translations and rotations), instead, is not so straightforward. These constraints depend on the site subgroup $\boldsymbol{G}_{\text{site}}$, which is formed by all symmetry operators $\hat{\boldsymbol{G}}_m$ leaving the site unchanged (i.e., leaving the center of mass unchanged). $\boldsymbol{G}_{\text{site}}$ is a subgroup of both crystallographic space group $\boldsymbol{G}_{\text{crystal}}$ and molecular point group $\boldsymbol{G}_{\text{molecule}}$ and completely determines the allowed displacements. Molecules on a crystallographic inversion site, for example, necessarily have a molecular inversion center at the same position. Since the center is fixed, all translations are forbidden, while any rotation is allowed.

In the general case, translation along an axis $\mathbf{t}$ or rotation around an axis $\mathbf{r}$ is forbidden if this would break the site symmetry. A symmetry operator $\hat{\boldsymbol{G}}_m$ acts as $\hat{\boldsymbol{G}}_m\mathbf{t} = \mathbf{G}_m\mathbf{t}$ or $\hat{\boldsymbol{G}}_m\mathbf{r} = |\mathbf{G}_m|\mathbf{G}_m\mathbf{r}$, where $\mathbf{G}_m$ is the 3×3 matrix describing the operator $\hat{\boldsymbol{G}}_m$ and $|\mathbf{G}_m| = \pm 1$ is its determinant. The difference between $\hat{\boldsymbol{G}}_m\mathbf{t}$ and $\hat{\boldsymbol{G}}_m\mathbf{r}$ is due to the fact that translations behave as normal vectors, while rotations do not change sign under inversion (they are pseudovectors). A translation along $\mathbf{t}$ does not break the site symmetry if $\mathbf{t}$ is unaffected by site operators, i.e., if $\hat{\boldsymbol{G}}_m\mathbf{t} = \mathbf{t}$, where $m = 1, 2,..., M$ runs on all operators in $\hat{\boldsymbol{G}}_{\text{site}}$. Thus $\mathbf{t}$ belongs to Γ^0_{site}, the total-symmetric irreducible representation of $\hat{\boldsymbol{G}}_{\text{site}}$. By adapting the method developed by Bernardinelli and Flack[43] for "origin-free" crystals (discussed below), we identify the allowed translations using the projector operator[44,45] onto Γ^0_{site}, defined as $\hat{\boldsymbol{P}}_{\text{site}} = \sum_m \hat{\boldsymbol{G}}_m/M$. The 3×3 matrix of the projector $\hat{\boldsymbol{P}}_{\text{site}}$ for $\mathbf{t}$ is thus $\mathbf{P}^{\mathbf{t}}_{\text{site}} = \sum_m \mathbf{G}_m/M$. Since $\hat{\boldsymbol{P}}_{\text{site}}$ is idempotent (i.e., $\hat{\boldsymbol{P}}^2_{\text{site}} = \hat{\boldsymbol{P}}_{\text{site}}$), its only possible eigenvalues are 0 and 1. Eigenvectors $\mathbf{t}$ with eigenvalue 1 (i.e., $\hat{\boldsymbol{P}}_{\text{site}}\mathbf{t} = \mathbf{t}$) belong to Γ^0_{site} and correspond to directions of allowed translations. With the space group described in a system of axes defined by its principal symmetry elements, as in the *International Tables for X-ray Crystallography*,[39] the matrix $\mathbf{P}^{\mathbf{t}}_{\text{site}}$ is already

diagonal.[43] Eigenvalues and eigenvectors may be found by inspection of the diagonal elements of $\mathbf{P}^{\mathbf{t}}_{\text{site}}$, avoiding actual diagonalization.

Additional translational constraints may be imposed for origin-free crystals,[46] in which the cell origin is not fixed by symmetry.[43] Molecular translations in a $P1$ system with $Z = 1$, for example, though certainly allowed by symmetry, are pointless. In fact, they correspond to rigid translations of the whole crystal, which do not affect the energy. We suppress these irrelevant degrees of freedom by freezing translations along origin-free directions for the first (or only) molecule in the unit cell. Origin-free directions belong to the total-symmetric irreducible representation $\Gamma^0_{\text{crystal}}$ of the complete space group $\boldsymbol{G}_{\text{crystal}}$ and are found using the appropriate projector matrix $\mathbf{P}^{\mathbf{t}}_{\text{crystal}}$.

Finally, we find the allowed crystallographic rotation axes in the same way as the allowed translation axes, using the projector matrix $\mathbf{P}^{\mathbf{r}}_{\text{site}} = \sum_m |\mathbf{G}_m|\mathbf{G}_m/M$ instead of $\mathbf{P}^{\mathbf{t}}_{\text{site}}$. The corresponding molecular axes are also fixed at this stage. Molecules constrained to rotate on a single axis, for example, may only occur on crystallographic symmetry planes or axes, which necessarily coincide with a molecular symmetry plane or axis. This is enough to lock the appropriate pair of crystallographic and molecular directions.

2.5. Uniform Distribution of Molecular Rotations. Molecular orientations are most often described in terms of Euler's angles ψ, θ, and ϕ.[47,48] A uniform distribution of orientations in three dimensions (3D), which is necessary for an efficient sampling, unfortunately requires a rather cumbersome nonuniform distribution on ψ, θ, and ϕ.[46,49] The problem becomes more tractable if the molecular orientations are instead described in terms of quaternions which, for our purposes, are 4D vectors $\mathbf{q} = (q_0, q_1, q_2, q_3)$ yielding rotation matrices $\mathbf{R}(\mathbf{q})$ defined by quadratic functions of the components.[47,48] It may be verified that a uniform distribution of 3D rotations simply corresponds to a uniform distribution of quaternions on the surface of the unit 4D hypersphere $q_0^2 + q_1^2 + q_2^2 + q_3^2 = 1$. The obvious direct method[48] to obtain such a distribution, by using four independent variables to sample points inside a 4D hypercube, followed by rejection of unsuitable samples, on the average requires $128/\pi^2 \approx 13.0$ uniform variables to generate a 3D rotation and is thus extremely inefficient. Starting from a rejection method due to Marsaglia,[48,50] in a previous work[12] we devised a scheme requiring an average of $1 + 8/\pi \approx 3.55$ uniform variables to generate a unit quaternion. We have now found in computer graphics literature[51] an even better method which avoids rejections altogether, requiring only three uniform variables for each quaternion. In this method[51] one generates three independent variables uniformly distributed between 0 and 1, x_0, x_1, and x_2. From these one computes two auxiliary variables $r_1 = (1 - x_0)^{1/2}$ and $r_1 = (x_0)^{1/2}$, two uniformly distributed angles $\theta_1 = 2\pi x_1$ and $\theta_2 = 2\pi x_2$ and finally obtains the desired unit quaternion as $\mathbf{q} = (r_1 \sin \theta_1, r_1 \cos \theta_1, r_2 \sin \theta_2, r_2 \cos \theta_2)$.

2.6. Completeness of the Search. We assess the completeness of the search by adapting the "sight−resight" (or "capture−recapture") method[52] used to estimate population sizes in wildlife ecology. This method is based on the "birthday problem", where one asks the average number of people required to find a pair with the same birthday.[53,54] The problem is relevant to several random allocation and hashing algorithms analyzed by Knuth in his monumental work.[53] It may be shown[53,54] that if one samples uniformly, with replacement, from a population of size n, the number of trials required for the first repeated sampling of *some* individual has the expectation value $\bar{q} = 1 + Q(n)$, where $Q(n) = \sum_{k=1}^{n} n!/(n - k)!n^k$, with asymptotic expansion $Q(n) \sim (\pi n/2)^{1/2}$. To estimate an unknown population size, we invert the problem and keep sampling until an individual is sampled twice for the first time. If $\bar{q}$ is the required number of samples, the estimate for the population size is then $\bar{n} = 2\bar{q}^{\,2}/\pi$. In practice, rather than stopping at the first repeated minimum, we continue, effectively improving the statistics on $\bar{q}$. When the sampling distribution is nonuniform, as it happens in our case, $\bar{n}$ becomes a lower bound for the population size, since the average number of trials required for the first repeated sample decreases if some minima are more easily accessible.

3. Calculations

For α-6T we have generated 52000 initial configurations distributed among 16 structural classes with $Z' \leq 2$, which include all frequently occurring structural classes[26,37,38] consistent with the C_{2h} molecular symmetry. These classes, listed in Table 1, are identified by the space group and by the (x, y, z) Wyckoff coordinates of the independent molecular sites. From this information we derive the number Z of molecules in the unit cell, the site symmetry, and the appropriate constraints, all indicated in the table. For most classes all molecules have site symmetry 1 (generic sites), and thus *require* no translational or rotational constraints. Molecules with site symmetry $\bar{1}$ (inversion sites) cannot translate (three constraints) but may freely rotate. Molecules with site symmetry 2 or m (lying on C_2 symmetry axes or on mirror planes) translate only along the axis (two constraints) or within the plane (one constraint), respectively, and rotate only around a single axis (two additional constraints). Origin-free directions, which *allow* additional constraints to be imposed, occur in a few non-centrosymmetric space groups.[43] The resulting number of independent degrees of freedom, which depends on the lattice type, on the number Z' of independent molecules and on the total number of constraints, ranges from 6 to 18 and is also reported in the table. The class with $N_{\text{DOF}} = 18$ corresponds to $P\bar{1}$ structures with two independent molecules on generic sites, with six freely varying triclinic lattice parameters (a, b, c, α, β, γ) plus six additional degrees of freedom for each molecule (unconstrained translations and rotations). There are two classes with $N_{\text{DOF}} = 6$. One corresponds to $C2/c$ structures with a single independent molecule on a 2-fold axis at coordinates $(0,y,{}^1/_4)$, with four freely varying monoclinic lattice parameters (a, b, c, and β) and two additional degrees of freedom (translation along y and rotation around the b axis). The other class corresponds to *Pnma* structures with a single independent molecule on a mirror plane at $(x,{}^1/_4,z)$, with three freely varying orthorhombic lattice parameters (a, b, c) and three additional degrees of freedom (translations in the $x-z$ plane and rotation around the b axis).

The number of initial configurations in the various class is listed in Table 1. The potential energy of each configuration was minimized with WMIN,[55] subject to the appropriate constraints. Nearly 70% of the configurations failed to converge to bound states (i.e., to compact structures with negative potential energy) and were discarded. About 16% of the surviving structures were also discarded, due to instabilities detected by computing with IONIC[35] the lattice vibrational frequencies at the center and at the boundaries of the Brillouin zone. The frequencies $\nu_{\mathbf{K}}$ of a stable lattice must be real and positive for all wavevectors $\mathbf{k}$.[34] Nonpositive frequencies indicate that the system is at an unstable saddle point, rather than at an energy minimum.

Once the potential minima were found, we analyzed their structures with PLATON[56] to identify the space group,[57] to find

TABLE 1: Structural Classes Chosen for the Search, Identified by the Space Group and by the (x, y, z) Wyckoff Coordinates of the Independent Molecular Sites[a]

								no. of minima		
lattice type	space group	site coordinates	Z	site symmetry	axis	N_{DOF}	initial configurations	total	distinct	estimated
triclinic	$P1$ (C_1^1)	($\underline{x}$,$\underline{y}$,$\underline{z}$)	1	(1)	any	9	1000	290	89	65.5
		($\underline{x}$,$\underline{y}$,$\underline{z}$) (x, y, z)	2	(1,1)	any	15	2000	373	353	3155.2
	$\bar{P}1$ (C_i^1)	(0,0,0)	1	($\bar{1}$)	any	9	1000	304	55	30.0
		(x, y, z)	2	(1)	any	12	2000	623	399	391.5
		(x, y, z) (x, y, z)	4	(1,1)	any	18	4000	445	419	2572.8
monoclinic	$P2_1$ (C_2^2)	(x, $\underline{y}$, z)	2	(1)	any	9	1000	596	248	145.7
		(x, $\underline{y}$, z) (x, y, z)	4	(1,1)	any	15	6000	2413	2172	6867.6
	$P2_1/c$ (C_{2h}^5)	(0,0,0)	2	($\bar{1}$)	any	7	3000	1582	292	103.5
		(x, y, z)	4	(1)	any	10	6000	3287	2010	1363.0
		(x, y, z) (x, y, z)	8	(1,1)	any	16	3000	570	567	21788.3
	$C2/c$ (C_{2h}^6)	(0, y,$^1/_4$)	4	(2)	b	6	6000	625	295	86.8
		(x, y, z)	8	(1)	any	10	3000	69	66	1655.8
orthorhombic	$P2_12_12_1$ (D_2^4)	(x, y, $\underline{z}$)	4	(1)	any	9	2000	1341	460	214.2
	$Pna2_1$ (C_{2v}^9)	(x, y, $\underline{z}$,)	4	(1)	any	8	3000	1231	479	209.7
	$Pbca$ (D_{2h}^{15})	(x, y, z)	8	(1)	any	9	3000	399	184	105.5
	$Pnma$ (D_{2h}^{16})	(x,$^1/_4$, z)	4	(m)	b	6	6000	804	201	81.9

[a] Underlined coordinates, $\underline{x}$, $\underline{y}$, or $\underline{z}$, indicate origin-free directions, allowed by symmetry, but frozen to suppress irrelevant degrees of freedom. The number Z of molecules in the unit cell, their site symmetry, the allowed rotation axes ("any" or "b" only) and the number of degrees of freedom are also listed. For each class we indicate the number of initial configurations, the total number of minima including duplicates, the number of distinct minima, and the estimated lower bound for the number of distinct minima.

the reduced Niggli cell,[58] and to standardize the crystallographic coordinates as described by Parthé and Gelato.[59,60] This step is necessary since structures occasionally converge to minima whose actual symmetry (with reasonable accuracy) is higher than initially assumed. In these cases we repeated the energy minimization after imposing any additional constraint required by the increased symmetry.

Finally, we identified identical minima encountered more than once by comparing energies, densities, and structures. At this purpose, we used the distance comparison method.[36,61,62] For each individual structure i, we consider a reference molecule, its first 14 neighbors, and, if necessary, a few extra neighbors to complete a spherical coordination shell. We then list all interatomic distances between the reference molecule and its neighbors and compute a root mean square (rms) deviation between individual lists i and j. For α-6T we have found deviations either below 0.05 Å (between structures identical within our computational accuracy) or well above 0.1 Å (between distinct structures).

All calculations were performed on a low-end personal computer at 3.20 GHz, 32 bits. The accumulated processor time was 106 days. About 98% of the time was spent in energy minimization.

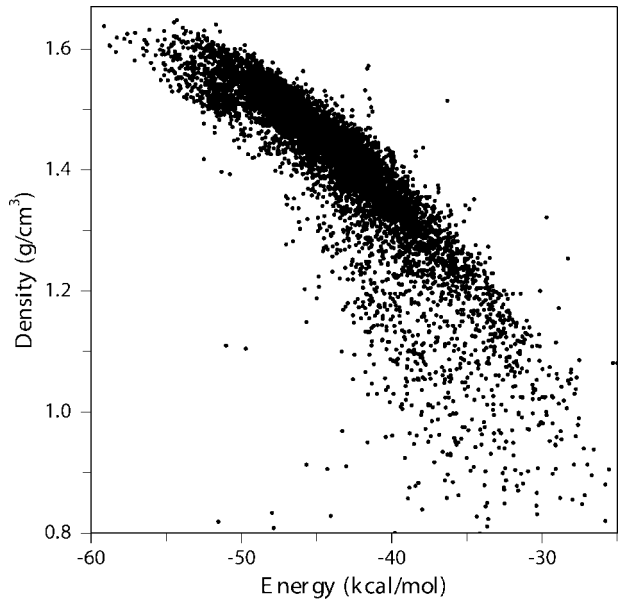

Figure 1. Density of the minima as a function of their energy.

4. Results and Discussion

4.1. Number of Minima. The search process produced about 15000 minima which, after identification of structures found more than once, reduced to over 7000 *distinct* minima spanning an energy range of about 30 kcal/mol. The energy as a function of the density, for all minima encountered in the search, is displayed in Figure 1. Beside the usual correlation between the two quantities,[12,15] it may be noticed that there is about a dozen deep minima, reasonably spread over a few kilocalories per mole, followed by a tight crowd of shallower minima. This is a practically important result, since the existence of a small number of deep equilibrium structures suggests that these should be resilient to minor perturbations in the potential model which, therefore, cannot be too critical.

The various structural classes chosen for the search, the number of initial configurations in each class, the total number of minima (including duplicates), the number of distinct minima (which do not necessarily belong to the initial class), and the lower bound for the number of distinct minima (estimated as discussed in section 2.6) are all listed in Table 1. The number of distinct minima and its estimated lower bound, which span 4 decades, are also compared in Figure 2.

Figure 2 shows that there are five structural classes (those appearing above the diagonal) for which the number of actually encountered distinct minima is well below the estimated lower bound. For these five classes, which include all structures with site symmetry (1,1) (two independent molecules on generic sites) and the $C2/c$ structures with site symmetry (1) (one independent molecule on a generic site), Table 1 indicates that almost all minima found during the search represent distinct minima or, equivalently, that very few minima have been encountered more than once. For the four structures with site symmetry (1,1), we attribute this behavior to the large dimensionality of the search space ($N_{DOF} \geq 15$), which, qualitatively, allows the existence

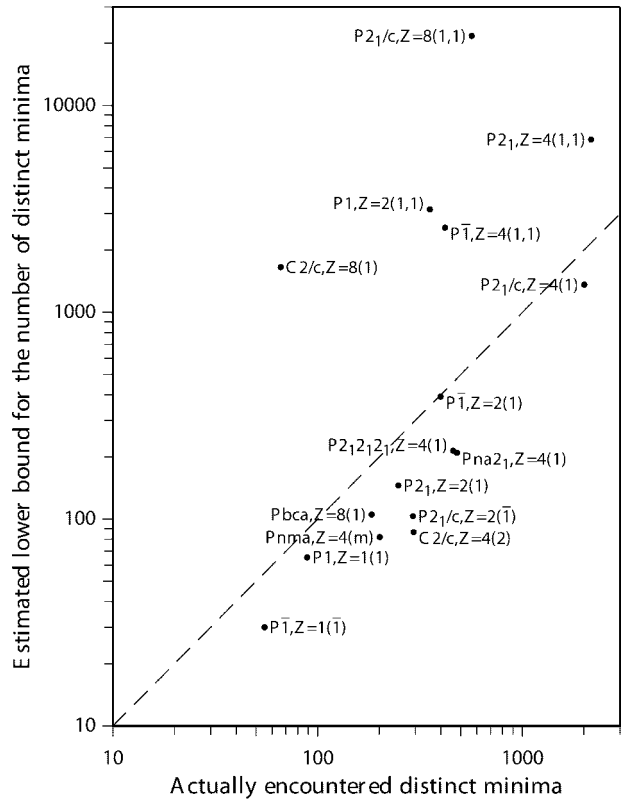

Figure 2. Number of actually encountered distinct minima compared to its lower bound number estimated with the "sight-resight" method, for all structural classes chosen for the search.

of many different minima. For the *C*2/*c* structures with site symmetry (1), either the dimensionality of the search space ($N_{DOF} = 10$) or the fact that most initial structures fail to reach stable configurations (as indicated by the table) may be relevant causes. For all five classes, since the average number $\bar{q}$ of minima to be sampled for a repeated encounter is large, the estimated lower bound for the number of distinct minima, $\bar{n} = 2\bar{q}^2/\pi$, is also large and, indeed, exceeds the number of minima actually encountered. In these conditions it is evident that the coverage of the search space is inadequate, because further searching would yield many more different minima. Rather than wasting computer time in the vain attempt of reaching a complete coverage, which would require computational resources orders of magnitude larger than those available to us, we have decided to truncate the search.

For all other structural classes (appearing below the diagonal in Figure 2), we might have instead identified a large part of the accessible minima. While sampling in these classes, in fact, we begin to approach a saturation plateau where to find new minima becomes progressively more difficult, because new configurations tend to fall more and more frequently onto previously encountered minima.

Although we cannot exactly pinpoint why some structures are so easy to search, it is clear that the reduced dimensionality of the search space is an important factor. In fact, we have empirically found that the estimated number of distinct minima $\bar{n}$ grows exponentially with the number of degrees of freedom since, with good approximation, $\log \bar{n}$ depends linearly on N_{DOF} (linear correlation coefficient[40] $r = 0.84$). Indeed, rather general arguments[63] indicate that the number of potential minima usually grows exponentially with the effective system size.

Another factor that may facilitate or hinder the search is the interaction between molecular and crystal symmetries. It has been shown that some space groups occur predominantly when molecules of suitable symmetry occupy special positions,[24,25] a regularity which may be rationalized by analyzing the effects of the various symmetry operators on the crystal packing. The molecular symmetry allows α-6T to occupy sites of symmetry $\bar{1}$, 2, or *m*, and this, in the appropriate space groups, facilitates the packing. For the space group *C*2/*c*, for example, we have encountered many structures with site symmetry 2 (Table 1), while, as already mentioned, most configurations starting from generic sites failed to reach stable structures.

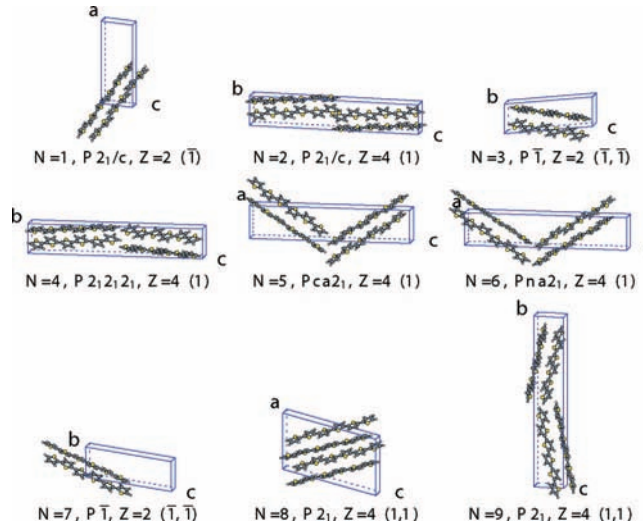

Figure 3. Structure of the nine deepest minima, shown with an orientation in which the shortest cell axis (either *a* or *b*) is approximately perpendicular to the plane of the page. Minima are labeled by their energy rank *N* (also indicated in Table 2) and structural class (space group, *Z*, and site symmetry). Graphics by Molscript.[64]

4.2. Structure of the Minima. Following the procedure used for pentacene[12] and tetracene,[15] we have classified the minima encountered during the search according to their structural class,[26,37] which is defined by the space group, by the number *Z* of molecules in the unit cell, and by the symmetry of the independent molecular positions (site symmetry) and thus completely characterizes the number and type of independent structural parameters.

A variety of structural arrangements have been found for α-6T, with triclinic, monoclinic, and orthorhombic lattices, in 45 different structural classes (covering 25 different space groups). By far the most common classes are $P2_1/c$ lattices with $Z = 4$ (1) (four equivalent molecules on generic sites) and $P2_1$ lattices with $Z = 4$ (1,1) (four molecules on two independent generic sites), both represented by thousands of structures. The structural classes chosen for the search and listed in Table 1 cover over 95% of the final structures. This is only partly due a tendency of the optimized structures to remain in the same class of the initial configuration, since over 25% of the structures actually changed class during the optimization. The most common of the remaining classes are $P\bar{1}$ lattices with $Z = 2$ ($\bar{1}$,$\bar{1}$) and $P2_1/c$ lattices with $Z = 4$ ($\bar{1}$,$\bar{1}$), both represented by about 80 structures, while all other classes are encountered only sporadically.

The structures of the nine deepest minima, chosen as typical examples of the structures encountered during the search, are drawn in Figure 3, while their molar potential energy, density, structural class, and crystallographic parameters are reported in Table 2. Among these nine minima we find seven different structural classes, a remarkable observation which is an indication of the surprisingly large variety of different packing

TABLE 2: Data for the Nine Deepest Minima[a]

N	space group	*Z*	site symmetry		Φ	ρ	*a*	*b*	*c*	α	*β*	*γ*
1	$P2_1/c$ (C_{2h}^5)	2	($\bar{1}$)	calcd	−59.1245	1.638	21.425	5.767	8.156	90.00	95.48	90.00
				exptl		1.553	20.672	5.684	9.140	90.00	97.78	90.00
2	$P2_1/c$ (C_{2h}^5)	4	(1)	calcd	−58.7812	1.606	5.960	7.661	45.171	90.00	97.29	90.00
				exptl		1.552	6.029	7.851	45.033	90.00	96.93	90.00
3	$P\bar{1}$ (C_i^1)	2	($\bar{1}$,$\bar{1}$)	calcd	−58.7347	1.605	5.958	7.669	22.678	84.63	82.97	89.35
4	$P2_12_12_1$ (D_2^4)	4	(1)	calcd	−58.3464	1.595	5.899	7.713	45.272	90.00	90.00	90.00
5	$Pca2_1$ (C_{2v}^5)	4	(1)	calcd	−58.2872	1.619	8.572	5.695	41.586	90.00	90.00	90.00
6	$Pna2_1$ (C_{2v}^9)	4	(1)	calcd	−57.7898	1.617	8.441	5.723	42.078	90.00	90.00	90.00
7	$P\bar{1}$ (C_i^1)	2	($\bar{1}$,$\bar{1}$)	calcd	−57.5780	1.625	5.717	7.870	22.729	96.87	94.20	92.66
8	$P2_1$ (C_2^2)	4	(1,1)	calcd	−57.3905	1.612	14.601	5.794	24.849	90.00	104.18	90.00
9	$P2_1$ (C_2^2)	4	(1,1)	calcd	−57.0834	1.581	5.902	44.460	7.985	90.00	97.10	90.00

[a] For each minimum, after the rank *N*, we report structural class (space group, *Z*, and site symmetry), molar potential energy Φ (kcal/mol), density ρ (g/cm^3), and lattice parameters (axes *a*, *b*, and *c* (Å); angles α, *β*, and *γ* (deg)). The reduced lattice parameters of the two known experimental polymorphs[22,23] are also reported.

arrangements. It has often been suggested[61,65] that this congestion of competing structures tends to hinder the efforts to find the global minimum. We like to point out that several deep minima ($N = 1$, 2, 4, 5, and 6), have only a single independent molecule ($Z' = 1$) but, due to symmetry, have two (or even four) molecules in the complete unit cell. Had we ignored all symmetry constraints, by sampling the space group $P1$ for structures with two (or four) independent molecules, we would have probably missed most of these minima due to the excessive size of the search space. The strategy of sampling many space groups while automatically exploiting all symmetry constraints (section 2.3) reduces the dimensionality of the search space and thus largely overcomes the sampling problem.

Once the potential minima were found, we compared them to the known experimental structures. We recall that for both pentacene and tetracene the two deepest minima were found to correspond to the two known experimental polymorphs.[12,15] For this reason, we are extremely thrilled to find that this happens also for α-6T. In fact, the two deepest potential minima are identical to the two energy minima analyzed in the previous paper[27] and obtained by starting from all known experimental structures.[21–23] The experimental structure of Siegrist et al.[23] converges to the deepest minimum ($N = 1$), while the two other X-ray structures[21,22] both converge to the next minimum ($N = 2$). The experimental lattice parameters[22,23] in the $P2_1/c$ standard setting, reported in Table 2, are well-matched by the calculations. The detailed comparison between experimental and computed structures, discussed in the previous paper[27] and not repeated here, is very satisfactory, especially when the effects of thermal expansion are taken into account with QHLD methods.[28]

5. Conclusions

We have presented the results of a systematic sampling of the potential energy hypersurface of crystalline sexithiophene (α-6T), performed to identify the possible polymorphs of this compound. Thousands of distinct minima have been encountered, with a large variety of structural arrangements. Among all these competing structures, as already found in our previous calculations for pentacene[12] and tetracene,[15] the two deepest minima correspond to the two known experimental[21–23] polymorphs. The finding that we have been able to predict all known experimental polymorphs of three different molecules, at the first attempt and with two different experimental polymorphs for each compound, clearly indicates that crystalline polymorphs *may be predictable*. For example, our approach should succeed also for α-4T, which experimentally presents a polymorphism[4,21] similar to that of α-6T.

The striking success of the predictions is highly significant, especially since the success rate in the blind tests in crystal structure prediction[36,61,66,67] is much lower. Indeed, we have participated in recent blind tests[36,67] and failed to predict any of the test structures.[36,67] Barring an unbelievable coincidence, there must be something special about tetracene, pentacene, and α-6T. Features shared by all three molecules, which may be reasons for their behavior, include high symmetry, quasi-rigid molecules with a single conformer, quasi-planar geometry, and highly delocalized π orbitals. A very interesting attempt[68] to identify which kinds of molecules have predictable crystal structures, in which nearly 200 prediction studies have been analyzed, did not produce a clear result. High-symmetry molecules with simple intermolecular interactions, in fact, seem to facilitate,[68] but by no means guarantee, successful predictions. In a recent investigation on tetracene,[69] we have found that the rank of the deepest minima is not affected if the electrostatic model is changed or even altogether discarded. This observation, which shows that the details of the potential model for tetracene are not very critical, suggests that packing constraints and short-range isotropic interactions largely control the structure and rank of the energy minima. This probably also hold for pentacene, α-6T, and other similar quasi-rigid molecules. For flexible or low-symmetry molecules, instead, we would expect an important role for highly anisotropic electrostatic interactions, such as dipole−dipole forces. Indeed, since the molecular geometry is kept fixed throughout the energy minimization, conformational polymorphism is outside the scope of our current treatment.

It may be noticed that all deep minima drawn in Figure 3, like all deep minima of pentacene and tetracene,[12,15] present close-packed herringbone structures which allow for significant electronic overlap between the π orbitals of neighboring molecules. This characteristic arrangement, which is claimed[7] to contribute to the excellent charge mobility properties of α-6T, may be due to a prevalence of isotropic intermolecular interactions.

The calculations for α-6T throw some light on the characteristics of the search space, which have important implications for the choice of the restart schedule.[70] In some search spaces, where many paths lead from anywhere to the global minimum, the starting point does not really matter. In other search spaces, where there are very few paths leading to the global minimum, one instead needs to restart many times trying to find one of these paths. This is clearly the case for α-6T, where the many-body energy hypersurface presents several deep distant minima separated by high barriers, as indicated by the computational evidence for a large number of different energy minima and by

the experimental identification of distinct polymorphs. The same holds for pentacene,[12] for tetracene,[15] and, probably, for many other molecular crystals. In these search spaces it is important to restart from many different initial configurations, as we have done by separately searching in the various space groups. Sampling as uniformly as possible, to ensure a good coverage of the search space while avoiding under- or oversampling, is also important. We have achieved this by adopting low-discrepancy sampling sequences[40,41] (which are optimally uniform) and by efficiently generating[51] uniform distributions of molecular orientations. We are very pleased with the overall behavior of our current search strategies, which, given a reliable potential model, seem really capable of identifying the deepest minima and, thus, the most stable polymorphs.

Acknowledgment. We thank Prof. William Porzio for helpful discussions. Work done with funds from MIUR (Grants PRIN 2003 and FIRB-RBNE01P4JF through INSTM consortium) and from the EU Integrated Project NAIMO (Project No. NMP4-CT-2004-500355).

References and Notes

(1) Reese, C.; Bao, Z. *Mater. Today* **2007**, *10*, 20–27.
(2) Park, Y. D.; Lim, J. A.; Lee, H. S.; Cho, K. *Mater. Today* **2007**, *10*, 46–54.
(3) Siegrist, T.; Kloc, C.; Laudise, R. A.; Katz, H. E.; Haddon, R. C. *Adv. Mater.* **1998**, *10*, 379–382.
(4) Antolini, L.; Horowitz, G.; Kouki, F.; Garnier, F. *Adv. Mater.* **1998**, *10*, 382–385.
(5) Ellern, A.; Bernstein, J.; Becker, J. Y.; Zamir, S.; Shahal, L.; Cohen, S. *Chem. Mater.* **1994**, *6*, 1378–1385.
(6) Mattheus, C. C.; Dros, A. B.; Baas, J.; Oostergetel, G. T.; Meetsma, A.; de Boer, J. L.; Palstra, T. T. M. *Synth. Met.* **2003**, *138*, 475–481.
(7) Garnier, F. *Acc. Chem. Res.* **1999**, *32*, 209–215.
(8) Dimitrakopoulos, C. D.; Malenfant, P. R. L. *Adv. Mater.* **2002**, *14*, 99–117.
(9) Karl, N. *Synth. Met.* **2003**, *133*−*134*, 649–657.
(10) Ruiz, R.; Choudhary, D.; Nickel, B.; Toccoli, T.; Chang, K. C.; Mayer, A. C.; Clancy, P.; Blakely, J. M.; Headrick, R. L.; Iannotta, S.; Malliaras, G. G. *Chem. Mater.* **2004**, *16*, 4497–4508.
(11) Venuti, E.; Della Valle, R. G.; Brillante, A.; Masino, M.; Girlando, A. *J. Am. Chem. Soc.* **2002**, *124*, 2128–2129.
(12) Della Valle, R. G.; Venuti, E.; Brillante, A.; Girlando, A. *J. Chem. Phys.* **2003**, *118*, 807–815.
(13) Brillante, A.; Bilotti, I.; Della Valle, R. G.; Venuti, E.; Masino, M.; Girlando, A. *Adv. Mater.* **2005**, *17*, 2549–2553.
(14) Venuti, E.; Della Valle, R. G.; Farina, L.; Brillante, A.; Masino, M.; Girlando, A. *Phys. Rev. B* **2004**, *70*, 104106/1–104106/8.
(15) Della Valle, R. G.; Venuti, E.; Brillante, A.; Girlando, A. *J. Phys. Chem. A* **2006**, *110*, 10858–10862.
(16) Stillinger, F. H.; Weber, T. A. *Phys. Rev. A* **1982**, *25*, 978–989.
(17) Della Valle, R. G.; Venuti, E.; Farina, L.; Brillante, A.; Girlando, A.; Masino, M. *Org. Electron.* **2004**, *5*, 1–6.
(18) Farina, L.; Syassen, K.; Brillante, A.; Della Valle, R. G.; Venuti, E.; Karl, N. *High Pressure Res.* **2003**, *23*, 349–354.
(19) Mattheus, C. C.; Dros, A. B.; Baas, J.; Meetsma, A.; de Boer, J. L.; Palstra, T. T. M. *Acta Crystallogr., Sect. C: Cryst. Struct. Commun.* **2001**, *57*, 939–941.
(20) Siegrist, T.; Besnard, C.; Haas, S.; Schiltz, M.; Pattison, P.; Chernyshov, D.; Batlogg, B.; Kloc, C. *Adv. Mater.* **2007**, *19*, 2079–2082.
(21) Porzio, W.; Destri, S.; Mascherpa, M.; Brükner, S. *Acta Polym.* **1993**, *44*, 266–272.
(22) Horowitz, G.; Bachet, B.; Yassar, A.; Lang, P.; Demanze, F.; Fave, J.-L.; Garnier, F. *Chem. Mater* **1995**, *7*, 1337–1341.
(23) Siegrist, T.; Fleming, R. M.; Haddon, R. C.; Laudise, R. A.; Lovinger, A. J.; Katz, H. E.; Bridenbaugh, P.; Davis, D. D. *J. Mater. Res.* **1995**, *10*, 2170–2173.
(24) Kitaigorodskii, A. I. *Organic Chemical Crystallography*; Consultants Bureau: New York, 1961.
(25) Brock, C. P.; Dunitz, J. D. *Chem. Mater.* **1994**, *6*, 1118–1127.
(26) Belsky, V. K.; Zorkii, P. M. *Acta Crystallogr., Sect. A: Found. Crystallogr.* **1977**, *33*, 1004–1006.
(27) Brillante, A.; Bilotti, I.; Biscarini, F.; Della Valle, R. G.; Venuti, E. *Chem. Phys.* **2006**, *328*, 125–131.
(28) Della Valle, R. G.; Venuti, E.; Brillante, A. *Chem. Phys.* **1996**, *202*, 231–241.
(29) Frisch, M. J.; Trucks, G. W.; Schlegel, H. B.; Scuseria, G. E.; Robb, M. A.; Cheeseman, J. R.; Montgomery, J. A., Jr.; Vreven, T.; Kudin, K. N.; Burant, J. C.; Millam, J. M.; Iyengar, S. S.; Tomasi, J.; Barone, V.; Mennucci, B.; Cossi, M.; Scalmani, G.; Rega, N.; Petersson, G. A.; Nakatsuji, H.; Hada, M.; Ehara, M.; Toyota, K.; Fukuda, R.; Hasegawa, J.; Ishida, M.; Nakajima, T.; Honda, Y.; Kitao, O.; Nakai, H.; Klene, M.; Li, X.; Knox, J. E.; Hratchian, H. P.; Cross, J. B.; Bakken, V.; Adamo, C.; Jaramillo, J.; Gomperts, R.; Stratmann, R. E.; Yazyev, O.; Austin, A. J.; Cammi, R.; Pomelli, C.; Ochterski, J. W.; Ayala, P. Y.; Morokuma, K.; Voth, G. A.; Salvador, P.; Dannenberg, J. J.; Zakrzewski, V. G.; Dapprich, S.; Daniels, A. D.; Strain, M. C.; Farkas, O.; Malick, D. K.; Rabuck, A. D.; Raghavachari, K.; Foresman, J. B.; Ortiz, J. V.; Cui, Q.; Baboul, A. G.; Clifford, S.; Cioslowski, J.; Stefanov, B. B.; Liu, G.; Liashenko, A.; Piskorz, P.; Komaromi, I.; Martin, R. L.; Fox, D. J.; Keith, T.; Al-Laham, M. A.; Peng, C. Y.; Nanayakkara, A.; Challacombe, M.; Gill, P. M. W.; Johnson, B.; Chen, W.; Wong, M. W.; Gonzalez, C.; Pople, J. A., *Gaussian03*, Revision D.02; Gaussian Inc.: Wallingford, CT, 2004.
(30) Lee, C.; Yang, W.; Parr, R. G. *Phys. Rev. B* **1988**, *37*, 785–789.
(31) Bayly, C. I.; Cieplak, P.; Cornell, W. D.; Kollman, P. A. *J. Phys. Chem.* **1993**, *97*, 10269–10280.
(32) Cornell, W. D.; Cieplak, P.; Bayly, C. I.; Kollman, P. A. *J. Am. Chem. Soc.* **1993**, *115*, 9620–9631.
(33) Cornell, W. D.; Cieplak, P.; Bayly, C. I.; Gould, I. R.; Merz, K. M., Jr.; Ferguson, D. M.; Spellmeyer, D. C.; Fox, T.; Caldwell, J. W.; Kollman, P. A. *J. Am. Chem. Soc* **1995**, *117*, 5179–5197.
(34) Born, M.; Huang, K., *Dynamical Theory of Crystal Lattices*; Oxford University Press: New York, 1954.
(35) Signorini, G. F.; Righini, R.; Schettino, V. *Chem. Phys.* **1991**, *154*, 245–261.
(36) Day, G. M.; Motherwell, W. D. S.; Ammon, H.; Boerrigter, S. X. M.; Della Valle, R. G.; Venuti, E.; Dzyabchenko, A.; Dunitz, J.; Schweizer, B.; van Eijck, B. P.; Erk, P.; Facelli, J. C.; Bazterra, V. E.; Ferraro, M. B.; Hofmann, D. W. M.; Leusen, F. J. J.; Liang, C.; Pantelides, C. C.; Karamertzanis, P. G.; Price, S. L.; Lewis, T. C.; Nowell, H.; Torrisi, A.; Scheraga, H. A.; Arnautova, Y. A.; Schmidt, M. U.; Verwer, P. *Acta Crystallogr., Sect. B: Struct. Sci.* **2005**, *61*, 511–527.
(37) Belsky, V. K.; Zorkaya, O. N.; Zorkii, P. M. *Acta Crystallogr., Sect. A: Found Crystallogr.* **1995**, *51*, 473–481.
(38) Mighell, A. D.; Rodgers, J. R. *Acta Crystallogr., Sect. A: Found. Crystallogr.* **1980**, *36*, 321–326.
(39) *International Tables for Crystallography: Space-Group Symmetry*, Vol. A; Hahn, Th., Ed.; Springer: Berlin, 2006.
(40) Press, W. H.; Teukolsky, S. A.; Vetterling, W. T.; Flannery, B. P. *Numerical Recipes in Fortran*; Cambridge University Press: Cambridge, U.K., 1992.
(41) Bratley, P.; Fox, B. L. *ACM Trans. Math. Software* **1988**, *14*, 88−100. Fortran77 source available at: NETLIB:http://www.netlib.no/netlib/toms/659.
(42) Kucherenko, S.; Sytsko, Y. *Comput. Optim. Appl.* **2005**, *30*, 297–318.
(43) Bernardinelli, G.; Flack, H. D. *Acta Crystallogr., Sect. A: Found. Crystallogr.* **1985**, *41*, 500–511.
(44) Cornwell, J. F. *Group Theory in Physics*; Academic Press: London, 1984.
(45) Atkins, P. W.; Friedman, R. S., *Molecular Quantum Mechanics*; Oxford University: Oxford, U.K., 1997.
(46) van Eijck, B. P.; Kroon, J. *Acta Crystallogr., Sect. B: Struct. Sci.* **2000**, *56*, 535–542.
(47) Allen, M. P.; Tildesley, D. J., *Computer Simulation of Liquids*; Clarendon: Oxford, U.K., 1987.
(48) Frenkel, D.; Smit, B., *Understanding Molecular Simulation: From Algorithms to Applications*; Academic Press: London, 1996.
(49) Dzyabchenko, A. V. *J. Struct. Chem.* **1984**, *25*, 416−420; **1984**, *25*, 559−563.
(50) Marsaglia, G. *Ann. Math. Stat.* **1972**, *43*, 645–646.
(51) Shoemake, K. *Graphics Gems III*; Academic Press: San Diego, CA, 1992; pp 124−132.
(52) Schnabel, Z. E. *Am. Math. Monthly* **1938**, *45*, 348–352.
(53) Knuth, D. E. *The Art of Computer Programming: Sorting and Searching*, Vol. 3; Addison-Wesley: Reading, MA, 1973.
(54) Flajolet, P.; Grabner, P. J.; Kirschenhofer, P.; Prodinger, H. *J. Comp. Appl. Math.* **1995**, *58*, 103–116.
(55) Busing, W. R.; Matsui, M. *Acta Crystallogr., Sect. A: Found. Crystallogr.* **1984**, *40*, 532–538.
(56) Spek, A. L. *J. Appl. Crystallogr.* **2003**, *36*, 7–13.
(57) Le Page, Y. *J. Appl. Crystallogr.* **1987**, *20*, 264−269; **1988**, *21*, 983−984.
(58) Santoro, A.; Mighell, A. D. *Acta Crystallogr., Sect. A: Found. Crystallogr.* **1970**, *26*, 124–127.
(59) Parthé, E.; Gelato, L. M. *Acta Crystallogr., Sect. A: Found. Crystallogr.* **1984**, *40*, 169–183.
(60) Gelato, L. M.; Parthé, E. *J. Appl. Crystallogr.* **1987**, *20*, 139–143.

(61) Lommerse, J. P. M.; Motherwell, W. D. S.; Ammon, H. L.; Dunitz, J. D.; Gavezzotti, A.; Hofmann, D. W. M.; Leusen, F. J. J.; Mooij, W. T. M.; Price, S. L.; Schweizer, B.; Schmidt, M. U.; van Eijck, B. P.; Verwer, P.; Williams, D. E. *Acta Crystallogr., Sect. B: Struct. Sci.* **2000**, *56*, 697–714.

(62) Chisholm, J.; Motherwell, W. D. S. *J. Appl. Crystallogr.* **2005**, *38*, 228–231.

(63) Stillinger, F. H. *Science* **1995**, *267*, 1935–1939.

(64) Kraulis, P. J. *J. Appl. Crystallogr.* **1991**, *24*, 946–950.

(65) Verwer, P.; Leusen, F. J. J. In *Reviews in Computational Chemistry*, Vol. 12; Lipkowitz, K. B., Boyd, D. B., Eds.; Wiley-VCH: New York, 1998; pp 327−365.

(66) Motherwell, W. D. S.; Ammon, H. L.; Dunitz, J. D.; Dzyabchenko, A.; Erk, P.; Gavezzotti, A.; Hofmann, D. W. M.; Leusen, F. J. J.; Lommerse, J. P. M.; Mooij, W. T. M.; Price, S. L.; Scheraga, H.; Schweizer, B.; Schmidt, M. U.; van Eijck, B. P.; Verwer, P.; Williams, D. E. *Acta Crystallogr., Sect. B: Struct. Sci.* **2002**, *58*, 647–661.

(67) Day, G. M.; Cooper, T. G.; Cabeza Cruz, A. J.; Hejczyk, K. E.; Ammon, H. L.; Boerrigter, S. X. M.; Tan, J.; Della Valle, R. G.; Venuti, E.; Jose, J.; Gadre, S. R.; Desiraju, G. R.; Thakur, T. S.; van Eijck, B. P.; Facelli, J. C.; Bazterra, V. E.; Ferraro, M. B.; Hofmann, D. W. M.; Neumann, M.; Leusen, F. J. J.; Kendrick, J.; Price, S. L.; Misquitta, A. J.; Karamertzanis, P. G.; W. A. Welch, G.; Scheraga, H. A.; Arnautova, Y. A.; Schmidt, M. U.; van de Streek, J.; Wolf, A.; Schweizer, B. *Acta Crystallogr., Sect. B: Struct. Sci.*, to be submitted for publication.

(68) Beyer, T.; Lewis, T.; Price, S. L. *CrystEngComm* **2001**, *44*, 178–212.

(69) Della Valle, R. G.; Venuti, E.; Brillante, A.; Girlando, A. *J. Phys. Chem. A* **2008**, *112*, 1085–1089.

(70) Fukunaga, A. S. *Lect. Notes Comput. Sci.*; **1998**, *1498*, 357 (http://www.bol.ucla.edu/~fukunaga/).

JP801749N